



Contents lists available at SciVerse ScienceDirect

Bone

journal homepage: www.elsevier.com/locate/bone

Original Full Length Article

Osteoblastic Wnts differentially regulate bone remodeling and the maintenance of bone marrow mesenchymal stem cells

Yong Wan^a, Cheng Lu^a, Jingjing Cao^a, Rujiang Zhou^a, Yiyun Yao^a, Jian Yu^a, Lingling Zhang^a, Haixia Zhao^a, Hanjun Li^a, Jianzhi Zhao^a, Xuming Zhu^a, Lin He^a, Yongzhong Liu^b, Zhengju Yao^a, Xiao Yang^c, Xizhi Guo^{a,*}

^a Bio-X Institutes, Key Laboratory for the Genetics of Developmental and Neuropsychiatric Disorders (Ministry of Education), Shanghai Jiao Tong University, Shanghai, 200240, China

^b State Key Laboratory of Oncogenes and Related Genes, Shanghai Cancer Institute, Shanghai, 200032, China

^c State Key Laboratory of Proteomics, Genetic Laboratory of Development and Disease, Institute of Biotechnology, Beijing 100071, China

ARTICLE INFO

Article history:

Received 29 August 2012

Revised 28 December 2012

Accepted 31 December 2012

Available online xxxx

Edited by: J. Aubin

Keywords:

Bone remodeling

Wnt

BMSCs

Osteoblast

Osteoclast

ABSTRACT

Wnt signaling has important roles in embryonic bone development and postnatal bone remodeling, but inconsistent impact on bone property is observed in different genetic alterations of *Lrp5* and β -catenin. More importantly, it is still controversial whether *Lrp5* regulate bone formation locally or globally through gut-derived serotonin. Here we explored the function of Wnt proteins in osteoblastic niche through inactivation of the *Wntless* (*Wls*) gene, which abrogates the secretion of Wnts. The depletion of *Wls* in osteoblast progenitor cells resulted in severe osteopenia with more profound defects in osteoblastogenesis, osteoclastogenesis and maintenance of bone marrow mesenchymal stem cells (BMSCs) compared to that observed in *Lrp5* and β -catenin mutants. These findings support the point of view that Wnt/*Lrp5* signaling locally regulates bone mass accrual through multiple effects of osteoblastic Wnts on osteoblastic bone formation and osteoclastic bone resorption. Moreover, osteoblastic Wnts confer a niche role for maintenance of BMSCs, providing novel cues for the definition of BMSCs niche in bone marrow.

© 2013 Elsevier Inc. All rights reserved.

Introduction

Postnatal bone remodeling requires an orchestrated action of osteoclastic bone resorption and osteoblastic formation in the basic multicellular unit (BMU) [1]. During this process, osteoblastic and osteoclastic activity is finely tuned by signals from the crosstalk between cells. For instance, osteoclasts release TGF- β factors from the bone matrix and recruit bone marrow mesenchymal stem cells (BMSCs) to the BMU [2]. Osteoblasts regulate osteoclast differentiation by secreting M-CSF, OPG and RANKL [3–8]. In addition, osteoblasts and osteoclasts are reciprocally modulated through the ephrinB2–EphB4 [9,10], Sema4D–Plexinb1 and Sema3A–Nrp1 signaling [11,12]. In contrast to these advances, little is known about how BMSCs are maintained and how they are activated to differentiate into osteoblasts in the BMU of bone remodeling.

Wnt signaling has extensive roles in regulating bone development and postnatal homeostasis based on a number of genetic alterations in components of Wnt signaling cascade [13–19], such as *Lrp5* and β -catenin. Loss-of-function mutation in *Lrp5* leads to osteoporosis [20], whereas gain-of-function mutation in *Lrp5* results in high bone mass [21–23]. Studies of other components of the canonical Wnt signaling cascade, such as β -catenin and Axin, indicate that Wnt signaling promotes bone formation through a variety of mechanisms, including

the stimulation of pre-osteoblast proliferation, induction of osteoblast differentiation and prevention of osteoblast and osteocyte apoptosis [13,14,24–26]. β -Catenin, the central effector of canonical Wnt signaling, prevents osteoclastic bone resorption by stimulating OPG expression in osteoblasts [3–5]. Recently, β -catenin in osteoclasts is also shown to cell-autonomously regulate osteoclastogenesis in a biphasic and dosage-dependent manner [27].

Despite the great progress, the impact and underlying mechanism of *Lrp5* in bone mass regulation are still controversial. Based on the observations in mice with osteocyte-specific alterations of *Lrp5*, or in compound mutant mice with limb mesenchyme-specific deficiency of *Lrp5* and *Lrp6* [16], *Lrp5* regulate bone mass accrual in a cell-autonomous manner. However, Yadav et al. detected no change in bone mass when *Lrp5* was inactivated in mature osteoblasts, whereas he observed a decrease of bone mass at loss of *Lrp5* in gut [28]. Therefore, the author suggests that *Lrp5* globally controls bone mass through an endocrine action of gut-derived serotonin, but not in the bone marrow. Genetic studies of the mutant mice devoid of individual Wnt ligand had provided no clear answer for this argument [29–32]. On the other hand, several types of cells in bone marrow, including osteoblasts and osteoclasts, secrete Wnt ligands [33]. In adult bone, Wnt5a has a role to coordinate osteoblast and osteoclast differentiation [34], and Wnt10b regulates BMSC maintenance in an age-dependent manner [17]. However, which type of cells produce Wnt proteins that are important for postnatal bone homeostasis remains elusive.

* Corresponding author.

E-mail address: xzguo2005@sjtu.edu.cn (X. Guo).

Recently, two SNP in *Wntless* locus are identified to be associated with reduced bone mass by genome wide association studies [35,36]. The *Wntless* (*Wls*), a transmembrane protein, is specifically required for the secretion of both canonical and non-canonical Wnt proteins in cells [37,38]. The mice with conventional inactivation of *Wls* die at embryonic stage with defects in the embryonic axis [39]. Conditional depletion of *Wls* has been extensively used to investigate the paracrine effect of Wnt proteins in a variety of tissues, including brain [37], limb, hair follicle epithelium [40] and mature osteoblasts [41]. In this study, we explored the role of Wnt proteins in postnatal bone remodeling through inactivating *Wls* gene in osteoblast progenitor cells. Our investigations support the point of view that osteoblastic Wnts locally regulate bone mass accrual through their combinatory effect on osteoblastic bone formation and osteoclastic resorption. Our findings also suggest that osteoblastic Wnts sustain maintenance of BMSCs, providing novel cues for identification of the BMSCs niche in bone marrow environment.

Materials and methods

Mice

The *Col1-cre* transgenic mice [42], *Osteocalcin-Cre* mice [43,44], *Wls^{c/c}* mice [38], and β -*cat^{ex3/+}* mice [45] were used as described. Each conditional knockout mouse was generated by a cross of *Col1-Cre* or *Osc-Cre* mice with *Wls^{c/c}* and β -*cat^{ex3/+}* mice. The genetic backgrounds of all mice were uniform mixtures of 129S1/SvIMJ and C57Bl/6J. All animal procedures were performed in accordance with guidelines set by Bio-X Institutes in Shanghai Jiao Tong University.

Calvarial cell culture and ALP staining

Osteoblasts were isolated from calvaria of newborn mice. Then soft tissue was removed and the calvaria were chopped into small fragments. The calvaria were then subjected to five sequential digestions with 0.05% Trpsin-EDTA (Gibco) and 0.5 mg/ml collagenase (Gibco) in α -MEM (Gibco) medium at 37 °C for 15 min each. The cells from the last four digestions were collected and cultured for subsequent experiments. In 24-well plates, 5×10^4 cells were seeded in each well and transferred into osteogenic medium containing 10 mM β -glycerol phosphate (Sigma), 50 μ g/ml ascorbate-2-phosphate (Sigma) and 10^{-7} M dexamethasone (Sigma) after reaching subconfluence. The culture medium was changed every other day for up to one week. Then ALP (Takara) staining was conducted according to the manufacturer's instruction.

Immunohistological and histomorphometric analyses

Before the bone samples were embedded in paraffin, the bones of P7 or P14 were fixed in 4% PFA at 4 °C overnight, and then decalcified in 15% EDTA for 7 days before H&E (Beyotime), Trap (Sigma), Safranin O staining. The embryonic skeletons of E17.5 for von Kossa staining were processed without decalcification. For histomorphometry, 10-mm-thick longitudinal sections were cut through the trabecular region. The primary antibodies used in the immunohistochemistry experiments were the following: anti-Wnt5a (R&D), anti-Wnt5b (Abgent), anti-Wnt10b (Sigma), anti-Osterix (Abcam), anti-Nestin (Abcam) and anti-BrdU (Abcam). The secondary antibodies used were the Alexa Fluor 488 conjugated and the Alexa Fluor 488 conjugated second antibody (Invitrogen). Mice received an intraperitoneal injection of bromodeoxyuridine (BrdU) (Sigma) with a dose of 100 μ g/g body mass, and were killed 2 h later, and then embedded in paraffin for sectioning. For primary calvarial cells, 5×10^4 primary calvarial cells were seeded in a 24-well plate and cultured for 24 h. Complete medium with 10 μ M BrdU (Sigma) was changed and incubated for 2 h. For BrdU incorporation and Tunel staining, sections or calvarial cells were treated according to the manufacturer's instructions.

Microcomputed tomography (μ CT)

Tibias were stripped of soft tissue and preserved in 70% EtOH at 4 °C. The bones were scanned in deionized water using a Micro-computed Tomography analysis system (Skyscan), images acquired at 50 kVp, 200 μ A, 280-ms integration time with voxel size of 18.26 μ m. Data were analyzed using Skyscan CT-analyzer software according to the guidelines described [46]. Quantitative morphometry data were based on region of interest (ROI) as following: trabecular bone region starting from growth plate reference level extending 44 slices (0.8 mm) distally, while cortical bone starting from mid-diaphysis extending 22 slices (0.4 mm) proximally. Quantitative morphometry data were qualified including: (1) bone volume fraction (BV/TV); (2) specific bone surface (BS/BV); (3) trabecular number (Tb.N); (4) trabecular bone mineral density (trabecular BMD); (5) average trabecular thickness (Tb.Th); and (6) trabecular separation (Tb.Sp); (7) average cortical thickness (Ct.Th).

RNA extraction and quantitative real-time PCR

RNA was extracted from cultured cells using the Trizol reagent (Invitrogen) according to standard procedures, while RNA was extracted from the long bone with a subtle adjustment: the long bones were crushed in liquid nitrogen, and further homogenized with a homogenizer. SuperScriptIII Reverse Transcriptase (Invitrogen) was used to reverse-transcribe 800 ng of RNA. Real-time PCR was performed on ABI Prism 7500 Sequence Detection System (Applied Biosystems) using a SYBR Green Kit (Roche). The samples were normalized to Actin expression. All primer sequences could be found in Supplementary Table 1.

Flow cytometric assay and CFU-F assays

Bone marrow were flushed from long bones, and the BMSCs were identified with staining of Lin(ebioscience), CD31(ebioscience), CD45(ebioscience), CD29(ebioscience) and Sca1(ebioscience). The osteoclast progenitor was identified with staining of CD11b(ebioscience), B220(BD), CD3(ebioscience), c-Kit(ebioscience) and CD115(Biolegend). For CFU-F assays, bone marrow were flushed from long bone, 1.0×10^6 cells were seeded in a single well of a 6-well plate for duplicate assays and cultured according to the manufacturer's recommendations (Stem Cell Technologies).

Serology

Blood samples from 2-week-old WT and *Wls*-null mice were harvested at the time of euthanization, and serum was prepared. Serum cross-linked C-telopeptide (CTX), OPG and RANKL were measured using a RatLaps ELISA Kit (1RTL4000, Nordic Biosciences, Herlev, Denmark) following the manufacturer's instructions.

BMMs isolation and coculture experiment

Bone marrow cells were flushed from long bone of P8 mice. After lysis of red blood cells, the residual cells were resuspended in complete α -MEM and incubated with 5 ng/ml M-CSF. After 24 h, the floating cells were collected and cultured in complete α -MEM with 10 ng/ml M-CSF. After another 24 h, the adherent cells were flushed with complete α -MEM to obtain bone marrow monocyte (BMM) cells.

For coculture experiment, 1×10^5 osteoblast cells were isolated from calvaria of P8 mice and then seeded in 24-well plate. 1×10^5 BMM cells were seeded on osteoblast cells since after osteoblast cells were adhere to the plate. The complete α -MEM culture medium was supplemented with 10 ng/ml M-CSF and 50 ng/ml RANKL, and the medium was changed every day for 5 days before TRAP staining.

Statistical analysis

Results are given as means \pm standard deviations. Statistical analysis was performed using Student's *t* test. For Figs. 2–7 and S2–S5, **P*<0.05, ***P*<0.01 and ****P*<0.001 versus the WT or control.

Results

Multiple Wnt proteins are dynamically expressed in differentiating osteoblasts

To determine the effect of Wnt proteins in postnatal bone homeostasis, we first examined the expression of various Wnts in differentiating osteoblasts. Quantitative RT-PCR (qPCR) indicated that multiple Wnt genes, including non-canonical *Wnt4*, *Wnt5a*, *Wnt5b*, *Wnt7b* and *Wnt16* and canonical *Wnt10b*, were dynamically expressed in differentiating osteoblasts of calvarial or cortical bones (Fig. 1A). *Wnt4*, *Wnt7b* and *Wnt16* expression levels were relatively higher in the mature osteoblasts in cortical bones compared to the immature osteoblasts in calvarial bones (Fig. 1A). Immunohistochemistry (IHC) assay validated that the

canonical *Wnt10b*, as well as the non-canonical *Wnt5a*, was highly expressed in the osteoblasts of the periosteum and trabecular region of long bones at E16.5 (Figs. 1C–D). At P7 or P14 postnatal stage, *Wnt5b* and *Wnt10b* expression were highly maintained in osteoblasts of periosteum and trabecular bones (Figs. 1E, G, I), but the expression of *Wnt5a* decreased in the mature osteoblasts (arrow in Figs. 1D, H). *Wnt5b* expression was not only detected in the osteoblasts or osteocytes within the cortical bone, but also partially overlapped with Nestin⁺ BMSCs at the surface of endosteal (arrows in Fig. 1E). These observations suggest that osteoblasts are important sources secreting differential Wnt ligands in bone marrow environment.

Depletion of osteoblastic Wls results in osteopenia

To explore the impact of osteoblastic Wnts on bone mass regulation, the *Wntless* (*Wls*) gene was conditionally depleted in the osteoblastic lineage by crossing *Wls*^{cl/c} mice with the *Col1a1-3.6kb-Cre* (*Col1-Cre*) or *Osteocalcin-Cre* (*Osc-Cre*) transgenic mice. In line with previous reports [42,44], X-gal staining on bone sections from the *Col1-Cre*; *R26R* mice revealed that the Cre-mediated recombination in the *Col1-Cre*

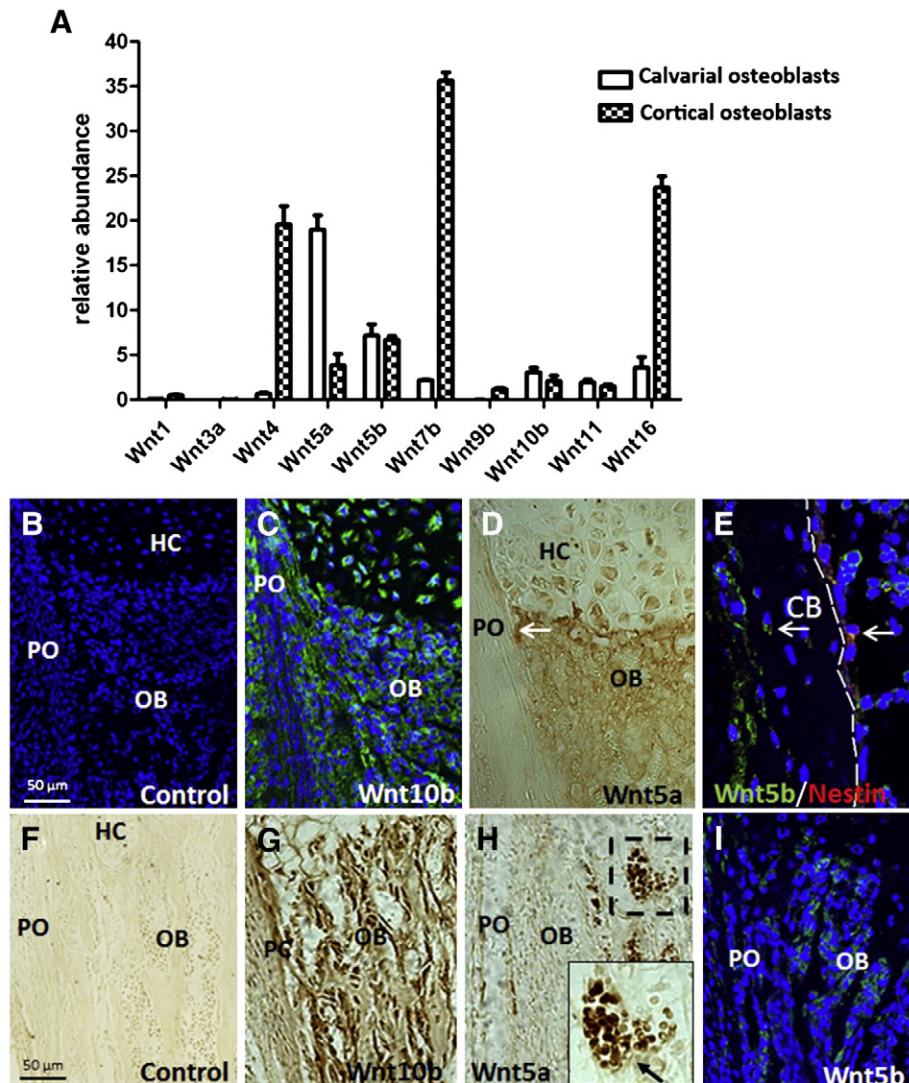


Fig. 1. Multiple Wnts are dynamically expressed in differentiating osteoblasts. A. The relative expression of Wnt genes in calvarial osteoblasts and cortical osteoblasts in wild-type (WT) mice as revealed by qPCR (*n*=3). B–I. The expression of *Wnt10b* (C, G), *Wnt5a* (D, H) and *Wnt5b* (E, I) in osteoblasts of the periosteum or the trabecular bone region during primary ossification at the E16.5 (B–D), P7 (E) and P14 (F–I) stages as detected by immunohistochemistry (IHC) examination. *Wnt5b* was also detected in osteoblasts within or at the endosteal surface of cortical bone (arrow in E). Nestin⁺ BMSCs (white arrows) was located in the vicinity of or overlapping with *Wnt5b*⁺ osteoblasts at P7 (arrow in E). The immature osteoblasts were isolated from calvaria while mature osteoblasts were from cortical bone at P8. The sections were obtained from distal femur (D, F–J) respectively. HC, hypertrophic chondrocytes; PO, periosteum; OB, osteoblast; TB, trabecular bone.

mice occurred at osteoblast progenitor stage (Fig. S1). The skeletal development in the *Col1-Cre; Wls^{c/c}* mice appeared largely normal at the prenatal stage except for a slightly delay in chondrocyte hypertrophy, as evidenced by skeletal preparations of the forelimb and hindlimb as well as Safranin O, H&E and von Kossa staining in sections at E17.5 (Fig. S2). However, a significant postnatal growth arrest was observed and most of the mutant mice died at one to two weeks of age (Figs. 2A and B), possibly due to heart failure (data not shown). Most of the *Col1-Cre; Wls^{c/c}* mice had defects at the skull ossification and vertebral organization (Figs. 2C, D). The axial skeletons were abnormally flexed at thoracic region, coupled with ectopic cartilage formation in the intervertebral disks and axial side of the ribs of the *Col1-Cre; Wls^{c/c}* mice (Figs. 2D, E).

Compared with the control littermates, the μ CT scan at P14 revealed that *Col1-Cre; Wls^{c/c}* mice had severe osteopenia, as evidenced by the marked decreases in the trabecular and cortical BMD, trabecular bone volume, trabecular bone number, trabecular and cortical bone thickness, and a concurrent increase in the trabecular BS/BV (Fig. 3). In contrast, depletion of *Wls* in mature osteoblasts in the *Osc-Cre; Wls^{c/c}* mice only displayed reductions in the cortical bone thickness, and had no changes in the other bone properties within the trabecular and cortical bone (Fig. S4). The *Osc-Cre; Wls^{c/c}* mice shown normal lifespan and were born at normal Mendelian frequency. These findings indicate that osteoblastic Wnts regulate bone mass accrual in a stage-dependent manner.

Osteoblastic Wnts promotes osteoblastogenesis in postnatal bone turnover

To understand the cellular basis of bone mass loss in the mutant mice, we first examined the proliferation and apoptosis of osteoblasts. Histomorphometric analysis based on H&E staining showed that the *Col1-Cre; Wls^{c/c}* mice had fewer osteoblasts per trabecular bone area

compared with the wild-type (WT) controls (Figs. 4A–C). In the consecutive bone sections, fewer BrdU-positive cells and more apoptotic osteoblasts were observed in the *Col1-Cre; Wls^{c/c}* mice according to the BrdU incorporation and TUNEL assay (Figs. 4D–I). These results indicate that osteoblastic Wnts sustain osteoblast proliferation and survival.

To investigate the osteoblast differentiation in the *Col1-Cre; Wls^{c/c}* mice, we examined the gene expression of osteoblast markers in the cortical bone using qPCR. The expression levels of *Runx2* and *Osterix* were not significantly altered (Fig. 4J), suggesting the initial osteoblast differentiation was not affected. However, further osteoblast differentiation and maturation was perturbed as evidenced by expression levels of late osteoblast markers, *Col1a1* and *Osteocalcin*, were remarkably downregulated in the mutants compared to the WT (Fig. 4J). In addition, the impairment in osteoblast differentiation was validated by alkaline phosphatase (ALP) staining in the osteogenic culture of primary calvarial cells obtained from neonatal mice (Fig. 4K). As evidenced by the decrease in *Leff1* transcript and β -catenin protein level at loss of *Wls* in primary calvarial cells (Figs. 4L–N), the canonical Wnt signaling activity was significantly downregulated in the mutant mice. These findings indicated that osteoblastic *Wls*-deficiency impairs bone formation through blocking the canonical Wnt signaling activity in the osteoblast lineage itself. Osteoblastic Wnts promote osteoblastogenesis through stimulating the osteoblast differentiation, proliferating and survival.

Ablation of osteoblastic Wls enhances osteoclast differentiation

To explore the osteoclastic bone resorption in the osteoblastic *Wls*-deficient mice, we examined the osteoclastogenesis through FACS analysis and TRAP staining. The osteoclast progenitors or precursors can be defined as $CD11b^+B220^-CD3^-CD117^+CD115^+$ [47]. FACS

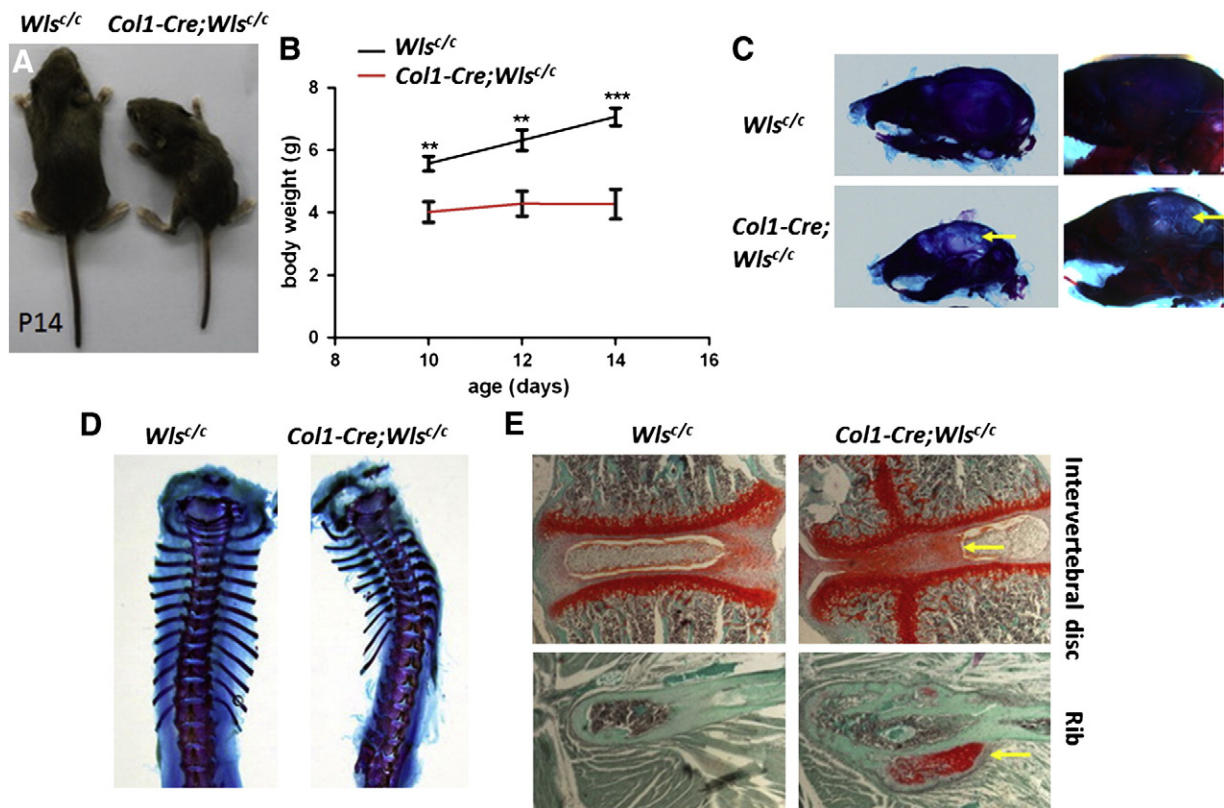


Fig. 2. Ablation of *Wls* in osteoblasts impairs the axial skeleton development. A. The *Col1-Cre; Wls^{c/c}* mice were much smaller in size compared with the WT littermates at P14. B. The growth curve of *Col1-Cre; Wls^{c/c}* mice exhibited obvious growth arrest after P10. C. The skull ossification was perturbed in the knockout mice as marked by arrows. D. The vertebrae were abnormally flexed in thoracic region. E. Ectopic cartilage chondrocytes were detected in the intervertebral disk and paraxial side of ribs in the mutant mice, as stained by Safranin O (yellow arrows). (For interpretation of the references to color in this figure legend, the reader is referred to the web version of this article.)

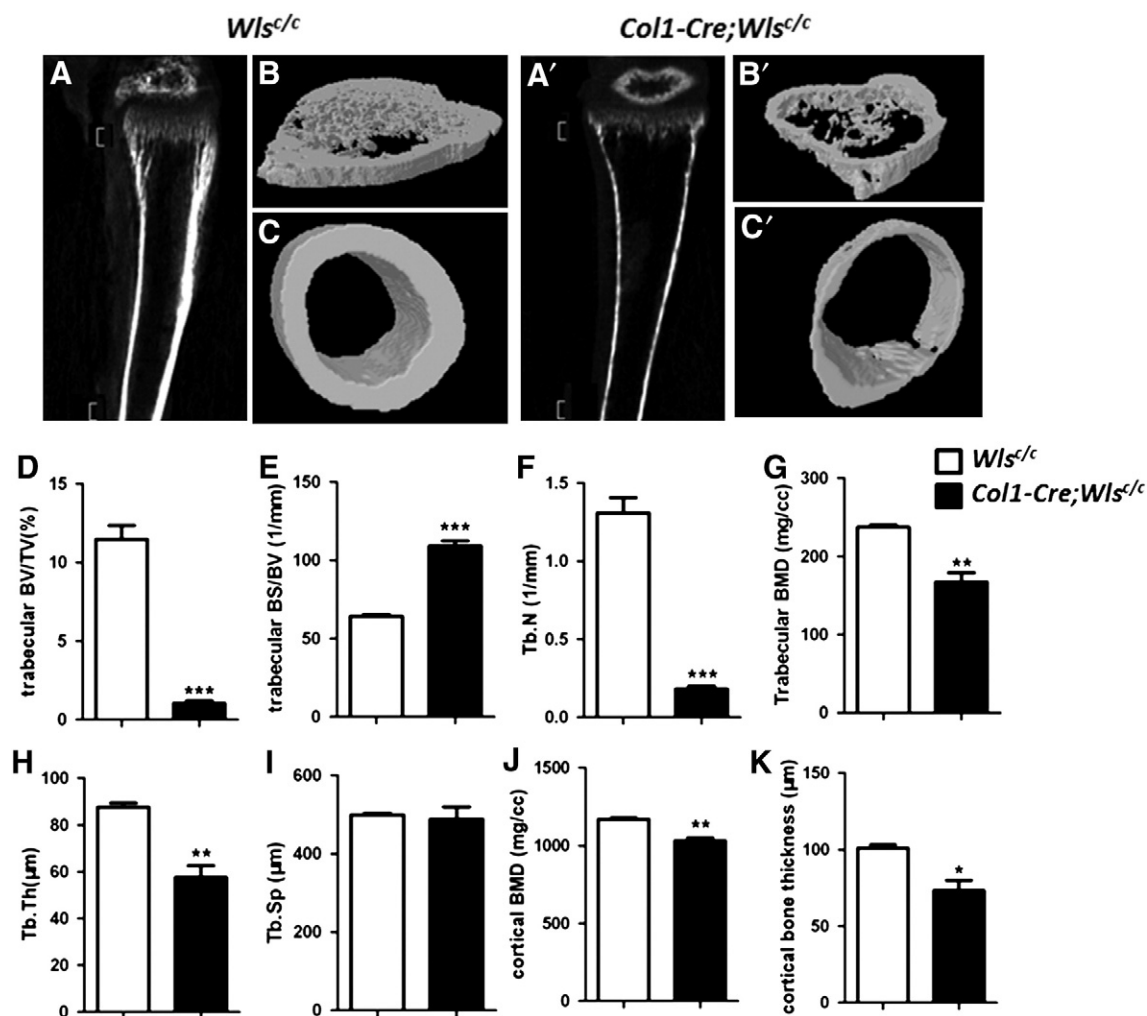


Fig. 3. μ CT scan for the bone mass accrual in the *Col1-Cre; Wls^{c/c}* mice. A–C'. The μ CT images of the tibia of P14 male mice. Sagittal sections were shown in (A, A') and 3-D images of the bracketed trabecular bones (B, B') and cortical bones (C, C') were shown. D–K. Graphs depicting the bone parameters in P14 (n = 3). The trabecular bone volume/total volume (BV/TV) (D), trabecular bone surface/bone volume (BS/BV) (E), trabecular number (F), trabecular BMD (G), trabecular thickness (H), trabecular separation (I), cortical BMD (J) and cortical bone thickness (K) were depicted.

analysis of bone marrow cells from long bones showed that the percentage of osteoclast progenitors had a significant increase in bone marrow of *Col1-Cre; Wls^{c/c}* mutant than the WT mice (Figs. 5A, B). In addition, TRAP staining indicated that the number of mature osteoclasts per trabecular bone area was also remarkably higher (Figs. 5C, D). These findings suggest that osteoblastic *Wls*-deficient mice have enhanced osteoclastic bone resorption.

OPG, RANKL and M-CSF, secreted by osteoblasts and osteocytes, are major regulators for osteoclastogenesis [48]. Therefore we measured the concentration of these proteins in serum by ELISA. The *Col1-Cre; Wls^{c/c}* mice at P14 expressed less OPG, more RANKL and had decreased OPG/RANKL ratio in serum compared to the controls (Figs. 5E, F and H). Meanwhile, the serum level of carboxy-terminal collagen crosslinks (CTX), a marker of bone resorption, was slightly elevated (Fig. 5G). The changes in the expression levels of *OPG*, *RANKL* and *M-CSF* genes were validated by qPCR examination in cortical bones (Fig. 5I). These alterations suggest that osteoblastic Wnts suppress osteoclastogenesis at least in part through modulating the expression of OPG, RANKL and M-CSF factors in osteoblasts.

The paracrine effect of osteoblastic Wnts on osteoclast differentiation

To assess the paracrine effect of osteoblastic Wnts on osteoclastogenesis, we generated *Col1-Cre; Wls^{c/c}; β -cat^{ex3/+}* mutant

mice with osteoblastic *Wls*-deficiency and a β -catenin gain-of-function allele. In the double mutant, endogenous Wnt/ β -catenin signaling was constitutively activated in osteoblasts whereas Wnt secretion was simultaneously blocked. The *Col1-Cre; β -cat^{ex3/+}* and *Col1-Cre; Wls^{c/c}; β -cat^{ex3/+}* double mutants died at around seven days of age, too small for analysis by μ CT scan. Therefore their osteoblastogenesis and osteoclastogenesis were examined through H&E and TRAP staining. The *Col1-Cre; Wls^{c/c}; β -cat^{ex3/+}* double mutants were similar in size as that of the *Col1-Cre; Wls^{c/c}* single knockout mice, but smaller than the WT controls at P7 (Fig. 6A). The *Col1-Cre; β -cat^{ex3/+}* mutant exhibited high bone mass with nearly abrogated osteoclastogenesis compared with the WT (Fig. 6F). The double mutant mice also had similar high bone mass as the *Col1-Cre; β -cat^{ex3/+}* mutant (Figs. 6C, D). However, the number of osteoclasts per trabecular bone area in the *Col1-Cre; Wls^{c/c}; β -cat^{ex3/+}* double mutant was partially restored compared to the *Col1-Cre; β -cat^{ex3/+}* single mutant (Figs. 6F, G and H). More importantly, the two mutants had comparable high *OPG* expression levels in osteoblasts with no apparent induction of *RANKL* and *M-CSF* genes (Fig. 6I).

To gain more insight into the regulation of osteoclast differentiation by osteoblastic Wnts, in vitro osteoclast formation assay was performed using bone marrow monocytes (BMMs) induced by RANKL/M-CSF. The osteoclast differentiation was assessed by TRAP staining after 5 days of culture. Without the osteoblast cocultures, RANKL/M-CSF-induced osteoclast differentiation were similar in BMMs between the *Wls^{c/c}* and

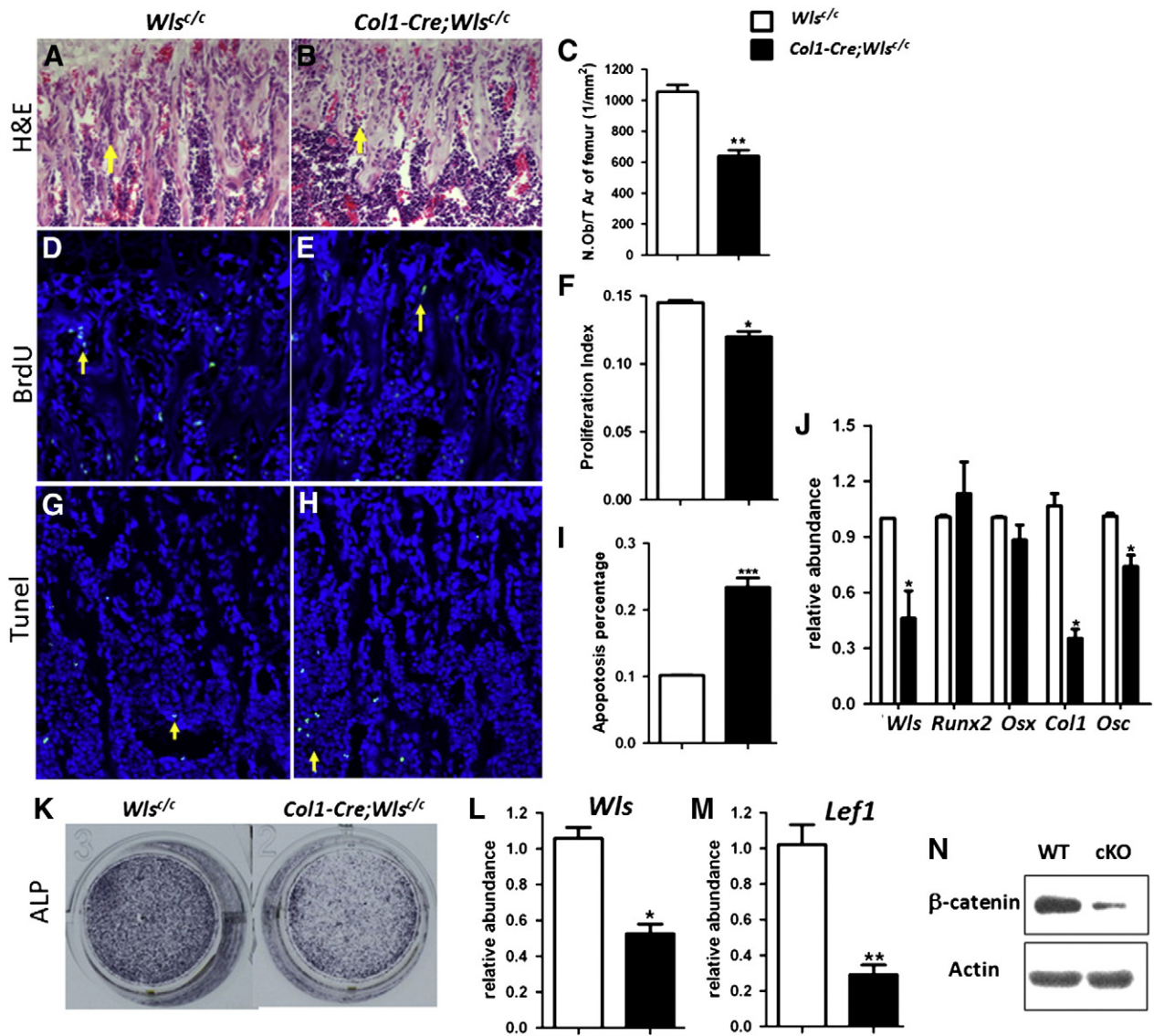


Fig. 4. Inactivation of *Wls* in osteoblasts impairs the osteoblastogenesis. A–H. H&E staining (A, B), BrdU labeling (D, E) and TUNEL staining (G, H) of the trabecular region of the distal femur of P14 mice. The osteoblasts were indicated by yellow arrows. Histomorphometric analysis (C) was conducted for the osteoblast number/tissue area (N.Ob/T.Ar) in the region shown in (A, B) ($n=3$). Statistical analysis of the osteoblast proliferation (F) and apoptosis (I) ($n=3$). J. Relative abundance of osteoblast markers in the cortical bone of P8 mice ($n=3$). Mature osteoblast differentiation was perturbed in the knockout mice, indicated by the decrease of *Col1* and *Osc* expression compared to controls. K. ALP staining in the calvarial osteogenic culture of neonatal calvarial osteoblasts. L–M. Relative abundance of *Wls* (L) and *Lef1* (M) in neonatal calvarial osteoblasts ($n=3$). N. Western blotting showed the lower level of β -catenin protein in neonatal calvarial osteoblasts compared to WT. (For interpretation of the references to color in this figure legend, the reader is referred to the web version of this article.)

Col1-Cre; Wls^{c/c} mice, indicated by the formation of comparable multinuclei osteoclasts (Figs. 7A, B). The osteoclast differentiation in the *Wls^{c/c}* BMMs was still similar, when cocultured with osteoblasts from the *Wls^{c/c}* mice or the *Col1-Cre; Wls^{c/c}* mice (Figs. 7C, D) under the influence of excessive RANKL/M-CSF stimulation. Interestingly, without RANKL/M-CSF treatment, mononuclear osteoclast differentiation from the *Wls^{c/c}* BMMs was still observed when cocultured with the *Col1-Cre; Wls^{c/c}* mutant osteoblasts, whereas no osteoclast formation was detected when cocultured with the *Wls^{c/c}* osteoblasts (Figs. 7C', D'). The difference in the osteoclastogenesis could not be fully explained by the action of *OPG/RANKL* axis, because the expressions of *OPG*, *RANKL* and *M-CSF* in feeder osteoblasts were not significantly changed between osteoblasts from WT and mutant (Fig. 7E). These experiments suggest that Wnt ligands from osteoblasts might have a paracrine effect in regulating osteoclast differentiation possibly through the direct interaction of osteoblastic Wnts on osteoclast cell

surface, as the way of osteoblastic Wnt5a that directly binds to the *Ror2* receptor in osteoclast cell surface [34].

Osteoblastic Wnts sustain BMSC maintenance

Interestingly, we observed that the *Wnt5b⁺* osteoblasts and the *Nestin⁺* BMSCs were partially overlapped or resided in the vicinity of the endosteal surface (white arrows in Fig. 1F). *Nestin* is recently considered to a marker for BMSCs [49]. It prompted us to investigate the effect of osteoblastic Wnts on BMSC maintenance. Through CFU-F assays in bone marrow, we observed a decrease in the colony number in bone marrow of the *Col1-Cre; Wls^{c/c}* mice compared to the control littermates (Figs. 8D, E). Additionally, the BMSCs could be enriched in the population gated by $\text{Lin}^- \text{CD31}^- \text{CD45}^- \text{CD29}^+ \text{Sca1}^+$ [2]. FACS analysis showed that the total number and proportion of BMSCs were decreased in the mutant compared to the WT (Figs. 8A–C).

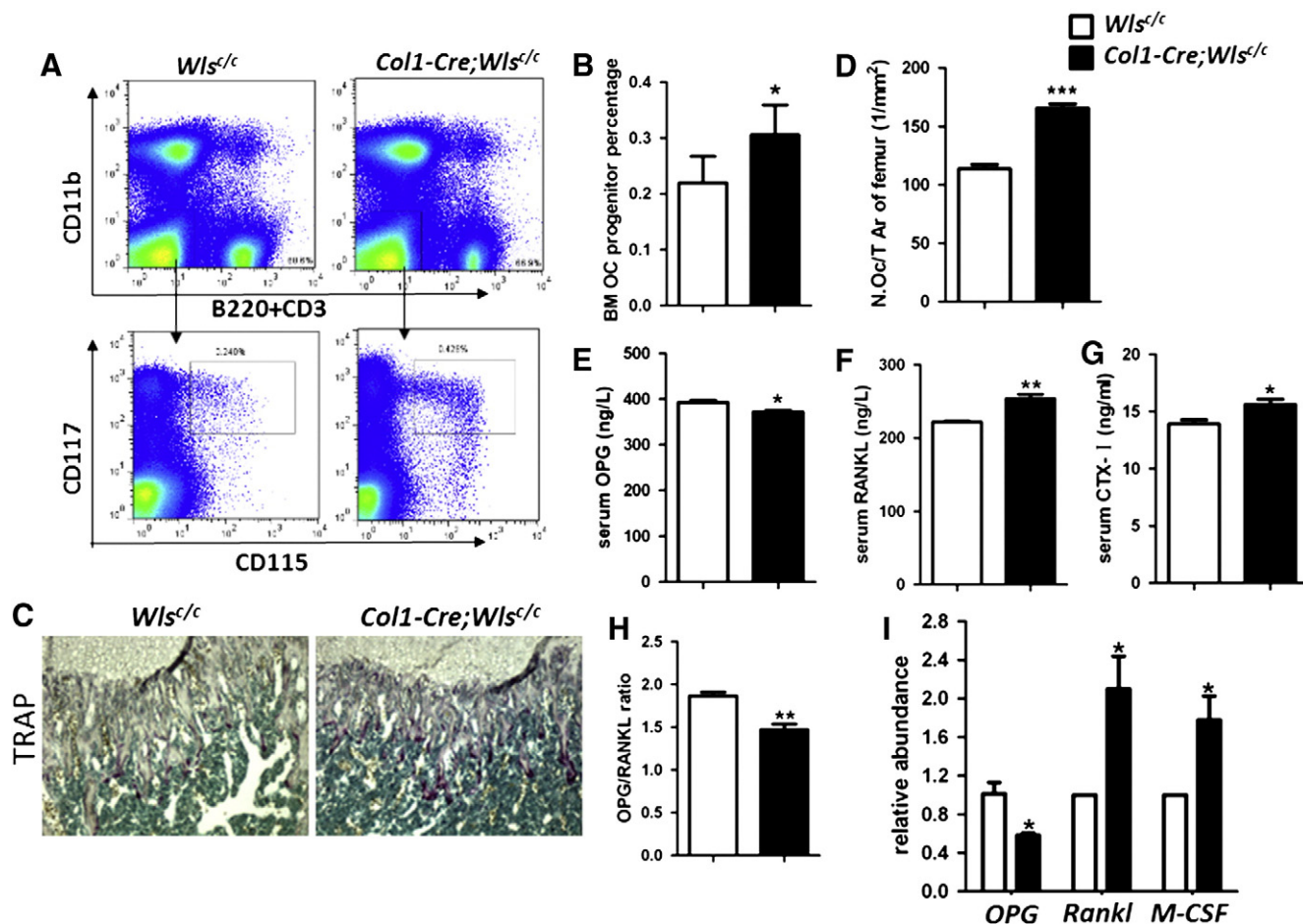


Fig. 5. Inactivation of *Wls* in osteoblasts enhances osteoclastogenesis. **A.** A representative FACS analysis of osteoclast progenitors in bone marrow from the WT and *Col1-Cre; Wls^{c/c}* mice at P8 stage. The osteoclast progenitor population was gated by CD11b⁺B220⁻CD3⁻CD117⁺CD115⁺. **B.** Graphs depicting the increased osteoclast progenitor percentage in the bone marrow (**A**) ($n=4$). **C.** TRAP staining of the trabecular region of the distal femur of P14 mice. **D.** Histomorphometric analysis of the osteoclast number/tissue area (N.Oc/T.Ar) in (**C**) ($n=3$). **E–G.** ELISA analysis of OPG (**E**), RANKL (**F**) and CTx (**G**) in the serum of P14 mice ($n=4$). **H.** Serum OPG/RANKL ratios of the samples in (**E, F**) ($n=4$). **I.** Relative abundance of *OPG*, *Rankl* and *M-CSF* genes in the cortical bone at P8.

Although it was not as definitive as the CFU-F assay, this analysis also revealed a niche role for osteoblastic Wnts in BMSC maintenance.

Discussion

In our study, we deplete *Wls* by osteoblast-specific *Cre*, which could examine the local action of Wnt proteins in osteoblastic niche and avoid function redundancy among Wnts. The osteoblastic *Wls*-deficiency mice had profound defects with decreased osteoblastogenesis, enhanced osteoclastogenesis and impaired maintenance of BMSCs in postnatal bone remodeling, combining deficiencies of that observed in osteoblast-specific *Lrp5* or β -catenin mutants [15,24–26,31]. These data support the notion that osteoblastic Wnts locally regulate bone remodeling through an array of mechanisms, including reciprocally promoting osteoblast differentiation and proliferation, suppressing osteoclast differentiation and maintaining BMSC self-renewal.

At the time of our manuscript preparation, a new report shows that a mature osteoblast-specific ablation of *Wls* by *Ocn-Cre* also resulted in similar and lesser severe defects in bone formation and resorption compared with our *Col1-Cre; Wls^{c/c}* mice [41]. The *Cre* activity in mature osteoblasts driven by a human *Osteocalcin* 10 kb promoter in the *Ocn-Cre* mice [50], is stronger than driven by a mouse 1.3 kb promoter in our *Osc-Cre* mice [44], but is later and more restricted than that in osteoblast progenitor cells affected by the *Col1-Cre* [42]. Therefore, the inactivation of *Wls* in osteoblast progenitor cells perturbed the osteoblast proliferation and survival (Fig. 4), which was not observed in mice with

depletion of *Wls* in mature osteoblasts by *Ocn-Cre* or *Osc-Cre* [41]. It is consistent with the notion that β -catenin signaling has important roles in promoting initial osteoblast induction, differentiation and proliferation during embryonic ossification process [24–26,31]. Taken together, these findings suggest that osteoblastic Wnts regulate osteoblastic bone formation in a context- and stage-dependent manner.

In fact, multiple Wnts expressions were observed in the osteoblastic niche, highlighting the heterogeneity of Wnt proteins in the bone remodeling microenvironment. Several Wnts including *Wnt5a*, *Wnt5b* and *Wnt16* were highly expressed in immature osteoblasts while *Wnt4*, *Wnt5b*, *Wnt7*, *Wnt10b* and *Wnt16* are expressed in mature osteoblasts (Fig. 1). *Wnt10b* is suggested to promote the osteoblastogenesis and suppress adipogenesis in mesenchymal progenitor cells [17,32]. On the other hand, *Wnt7b*, another non-canonical osteogenic Wnts (Fig. 1), has been demonstrated to promote osteoblast differentiation during prenatal skeletal ossification [30]. Meanwhile, the non-canonical *Wnt5a* also has similar role in committing osteoblast cell fate as *Wnt10b* [29]. Taken together, a variety of osteoblastic Wnts, including the canonical *Wnt10b* and non-canonical *Wnt5a*/*Wnt7b*, synergistically promote osteoblastogenesis and bone formation.

Osteoblasts have been revealed to regulate osteoclastogenesis through *OPG* induction by Wnt/ β -catenin in osteoblasts, or through direct binding of *Wnt5a* to its receptor on the surface of osteoclast progenitors [34]. Interestingly, inactivation of *Wls* in osteoblast progenitor cells enhanced osteoclastogenesis, coupled with alterations of *OPG* and *RANKL* expressions. The enhancement of osteoclastogenesis at loss of

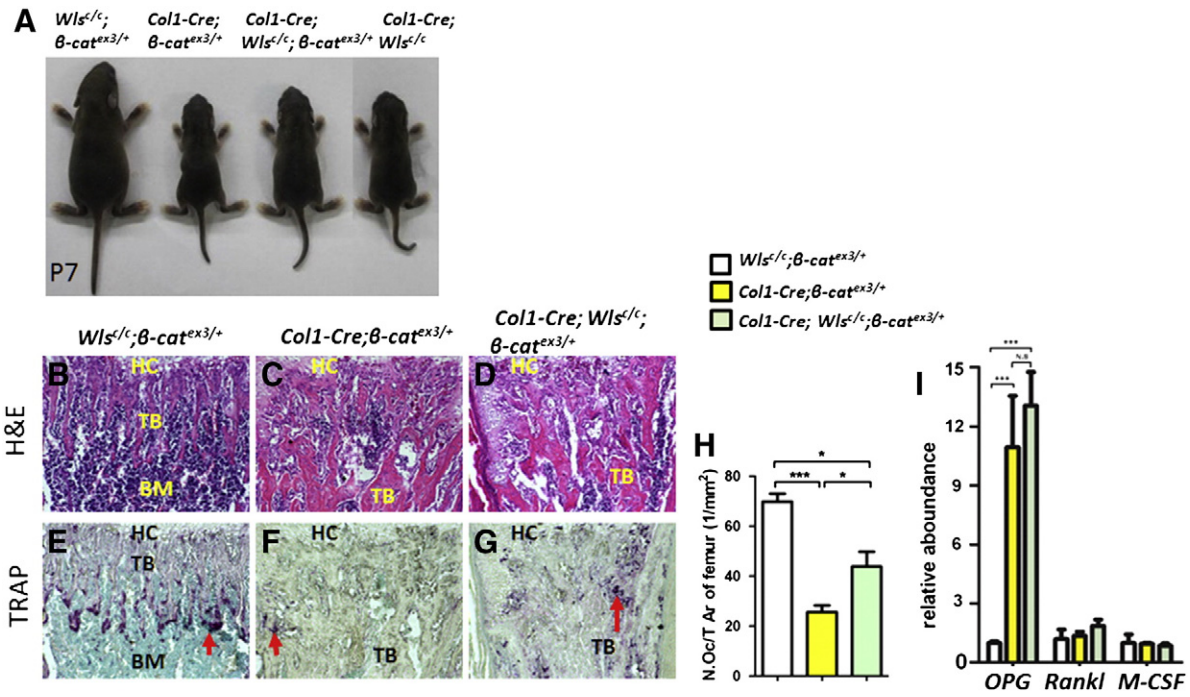


Fig. 6. Osteoclastogenesis is partially restored in the *Col1-Cre; $\beta\text{-cat}^{\text{ex3/+}}$; $Wls^{c/c}$* mice compared to the *Col1-Cre; $\beta\text{-cat}^{\text{ex3/+}}$* mice. **A.** Representative image for the WT, *Col1-Cre; $Wls^{c/c}$* , *Col1-Cre; $\beta\text{-cat}^{\text{ex3/+}}$* and *Col1-Cre; $\beta\text{-cat}^{\text{ex3/+}}$; $Wls^{c/c}$* mice at P7. The growth of the double mutant mice was not fully restored compared to the WT mice. **B–G.** H&E (**B–D**) and TRAP (**E–G**) staining for the trabecular region of the distal femur in these single and double mutant mice at P7. HC, hypertrophic chondrocyte; TB, trabecular bone; BM, bone marrow. **H.** Histomorphometric analysis of the osteoclast number/tissue area (N.Oc/T.Ar) in (**E–G**) ($n=3$). **I.** qPCR results of *OPG*, *RANKL* and *M-CSF* from the cortical bone of P7 mice ($n=3$). N.S., not significant.

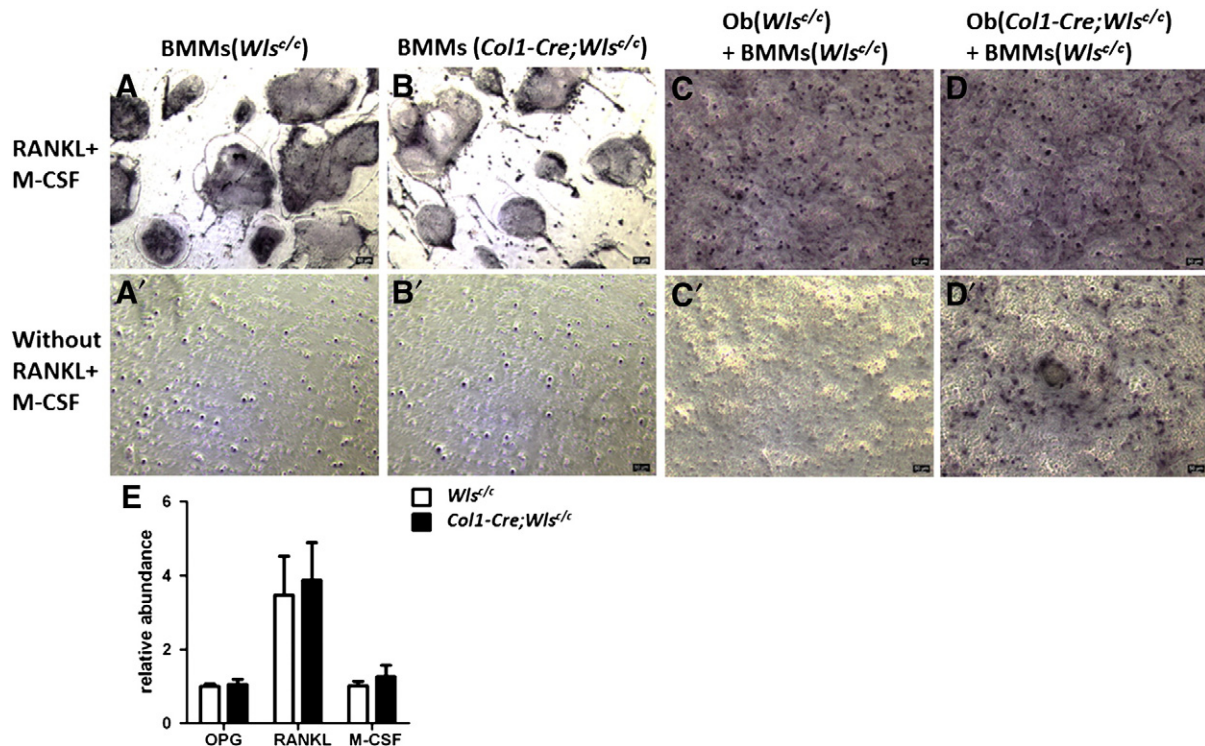


Fig. 7. Lack of osteoblastic Wnts enhances osteoclast differentiation without the stimulation of RANKL/M-CSF. TRAP staining was performed to assess osteoclast differentiation induced from bone marrow monocytes (BMMs) cocultured with or without osteoblasts. **A–A'.** Osteoclast differentiation in BMMs from the *Wls^{c/c}* mice at P8. **B–B'.** Osteoclast differentiation in BMMs from the *Col1-Cre; $Wls^{c/c}$* mice at P8. **C–C'.** Osteoclast differentiation in BMMs from the *Wls^{c/c}* mice at P8 cocultured with osteoblasts (Ob) from *Wls^{c/c}* mice at P8. **D–D'.** Osteoclast differentiation in BMMs from the *Wls^{c/c}* mice at P8 cocultured with osteoblasts from the *Col1-Cre; $Wls^{c/c}$* mice at P8. The culture medium was supplemented with (**A–D**) or without M-CSF and RANKL (**A'–D'**). **E.** qPCR results of *OPG*, *RANKL* and *M-CSF* from osteoblasts (Ob), isolated from calvaria of *Wls^{c/c}* mice and *Col1-Cre; $Wls^{c/c}$* mice at P8 ($n=3$).

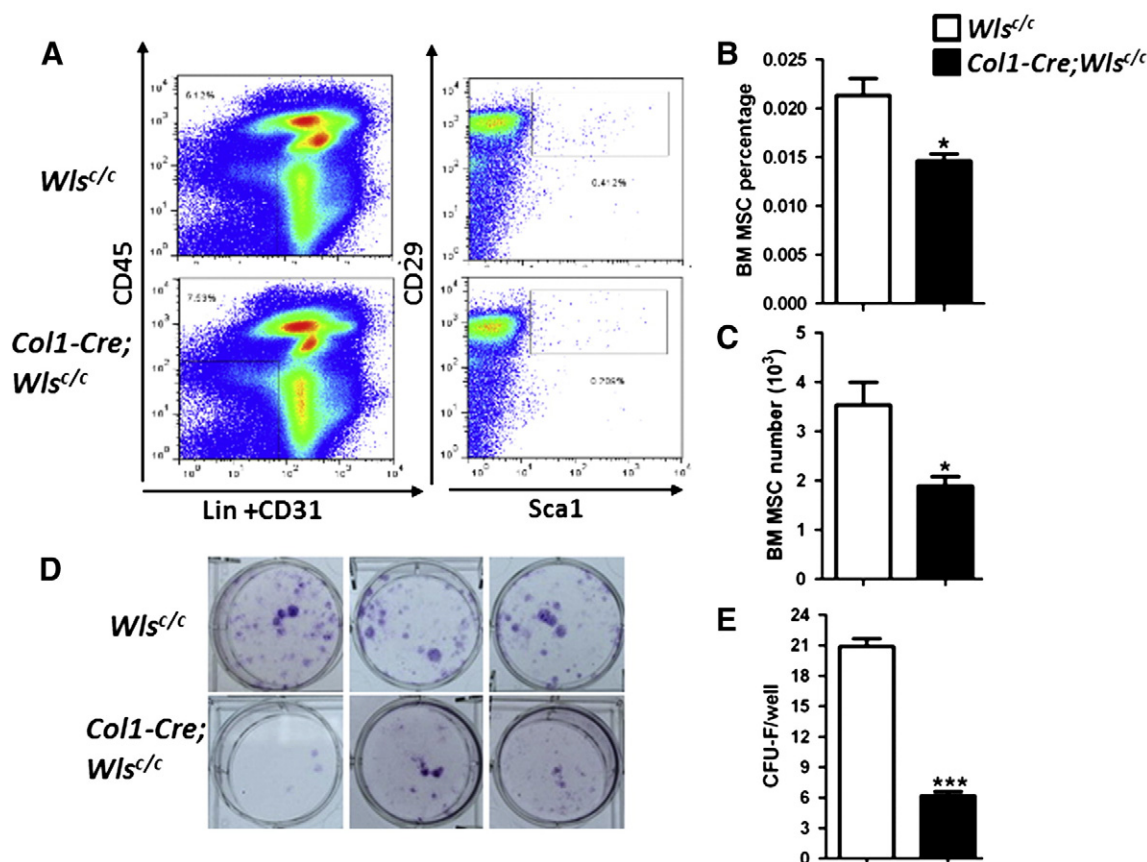


Fig. 8. Osteoblastic Wnts sustain self-renewal of BMSCs. A. A representative FACS analysis of the BMSCs in bone marrow. The BMSCs were gated by Lin⁻CD31⁻CD45⁻CD29⁺Sca1⁺. B–C. Graphs depicting the BMSC percentage (B) and total number (C) in bone marrow (n=4). D. CFU-F assay of the BMSCs in bone marrow. E. Score of the CFU-F colony number in (D) (n=3). Bone marrow cells were flushed out from the WT and *Col1-Cre; Wls^{c/c}* mice at P8–10 (A–D).

osteoblastic Wnts could be validated by in vitro osteoclast formation assay. Without excessive OPG/RANKL stimulation, osteoclast differentiation from BMMs still occurred when cocultured with osteoblasts from the *Col1-Cre; Wls^{c/c}* mice, but not in cocultures with osteoblasts from *Wls^{c/c}* mice (Figs. 7E, F), though the expressions of OPG, RANKL and M-CSF in osteoblast feeder layers were comparable. Additionally, in the double mutant mice with both osteoblastic *Wls*-deficiency and β -catenin gain-of-function, the arrest of osteoclastogenesis was partially rescued compared to the single mutant of *Col1-Cre; β -catenin^{ex3/+}*, while their high bone mass phenotypes and OPG expression were comparable between the two mutants (Fig. 6). Previous report has shown that *Col1-Cre (3.6kb)* mouse line has Cre activity in a limited population of osteoclast lineages in addition to osteoblasts [51]. Therefore, the defects at osteoclastogenesis might partially result from the lack of *Wls* in osteoclasts themselves, or from the *Wls* deficiency in osteoblasts. In a recent report, mature osteoblast-specific depletion of *Wls* by *Ocn-Cre* also led to an enhancement in osteoclast differentiation without alterations in OPG/RANKL axis [41]. These findings indicate that several Wnts from osteoblasts might function to suppress osteoclastogenesis in addition to OPG/RANKL axis. One possible mechanism is that the canonical Wnts secreted from osteoblasts directly regulate osteoclast differentiation, through activation of β -catenin signaling in osteoclast lineages [27].

Until now, our knowledge of the stem cell microenvironment in bone marrow has mainly focused on the hematopoietic stem cell (HSC) niche, which has been defined as the endosteal and vascular niche [52]. However, little is known about the BMSC niche or the cellular constituents for BMSC self-renewal and maintenance. Mice with osteoblastic *Wls*-deficiency had fewer colonies in CFU-F assay and smaller BMSC populations compared to the controls (Fig. 7). The identity of the

specific ligand for BMSC maintenance remains unclear. Wnt10b has been shown to have an age-dependent role in BMSC maintenance [17]. However, the loss of BMSCs in *Wnt10b*-null mice is progressive and less severe than that observed in the *Wls*-deficient mice. Therefore, we speculate that several osteoblastic Wnts other than Wnt10b sustain BMSC maintenance.

In summary, our findings suggest that osteoblastic Wnts locally and differentially regulate an array of biological activities in the bone remodeling, including osteoblastogenesis, osteoclastogenesis and BMSC maintenance. Wnts secreted from osteoblasts reciprocally promote osteoblastogenesis and bone formation, and suppress osteoclast differentiation in addition to OPG/RANKL axis. Importantly, we reveal that osteoblastic Wnts confer a niche role for BMSC maintenance, providing novel insights into definition of the BMSC niche.

Supplementary data to this article can be found online at <http://dx.doi.org/10.1016/j.bone.2012.12.052>.

Acknowledgments

This work was supported by the National Major Fundamental Research 973 program of China under grants [2007CB947301 and 2012CB966903] and by grants from the National Natural Science Foundation of China [31171396, 31271553, 81121001 and 31100624].

References

- Harada S, Rodan GA. Control of osteoblast function and regulation of bone mass. *Nature* 2003;423:349–55.
- Tang Y, Wu X, Lei W, Pang L, Wan C, Shi Z, et al. TGF-beta1-induced migration of bone mesenchymal stem cells couples bone resorption with formation. *Nat Med* 2009;15:757–65.

- [3] Glass II DA, Bialek P, Ahn JD, Starbuck M, Patel MS, Clevers H, et al. Canonical Wnt signaling in differentiated osteoblasts controls osteoclast differentiation. *Dev Cell* 2005;8:751–64.
- [4] Holmen SL, Zylstra CR, Mukherjee A, Sigler RE, Faugere MC, Bouxsein ML, et al. Essential role of beta-catenin in postnatal bone acquisition. *J Biol Chem* 2005;280:21162–8.
- [5] Kramer I, Halleux C, Keller H, Pegurri M, Gooi JH, Weber PB, et al. Osteocyte Wnt/beta-catenin signaling is required for normal bone homeostasis. *Mol Cell Biol* 2010;30:3071–85.
- [6] Spencer GJ, Utting JC, Etheridge SL, Arnett TR, Genever PG. Wnt signalling in osteoblasts regulates expression of the receptor activator of NFkappaB ligand and inhibits osteoclastogenesis in vitro. *J Cell Sci* 2006;119:1283–96.
- [7] Shin CS, Her SJ, Kim JA, Kim DH, Kim SW, Kim SY, et al. Dominant negative N-cadherin inhibits osteoclast differentiation by interfering with beta-catenin regulation of RANKL, independent of cell–cell adhesion. *J Bone Miner Res* 2005;20:2200–12.
- [8] Nakashima T, Hayashi M, Fukunaga T, Kurata K, Oh-Hora M, Feng JQ, et al. Evidence for osteocyte regulation of bone homeostasis through RANKL expression. *Nat Med* 2011;17:1231–4.
- [9] Zhao C, Irie N, Takada Y, Shimoda K, Miyamoto T, Nishiwaki T, et al. Bidirectional ephrinB2-EphB4 signaling controls bone homeostasis. *Cell Metab* 2006;4:111–21.
- [10] Irie N, Takada Y, Watanabe Y, Matsuzaki Y, Naruse C, Asano M, et al. Bidirectional signaling through ephrinA2-EphA2 enhances osteoclastogenesis and suppresses osteoblastogenesis. *J Biol Chem* 2009;284:14637–44.
- [11] Hayashi M, Nakashima T, Taniguchi M, Kodama T, Kumanogoh A, Takayanagi H. Osteoprotection by semaphorin 3A. *Nature* 2012;485:69–74.
- [12] Negishi-Koga T, Shinohara M, Komatsu N, Bito H, Kodama T, Friedel RH, et al. Suppression of bone formation by osteoclastic expression of semaphorin 4D. *Nat Med* 2011;17:1473–80.
- [13] Kato M, Patel MS, Levasseur R, Lobov I, Chang BH, Glass II DA, et al. Cbfa1-independent decrease in osteoblast proliferation, osteopenia, and persistent embryonic eye vascularization in mice deficient in Lrp5, a Wnt coreceptor. *J Cell Biol* 2002;157:303–14.
- [14] Bodine PV, Zhao W, Kharode YP, Bex FJ, Lambert AJ, Goad MB, et al. The Wnt antagonist secreted frizzled-related protein-1 is a negative regulator of trabecular bone formation in adult mice. *Mol Endocrinol* 2004;18:1222–37.
- [15] Cui Y, Niziolek PJ, MacDonald BT, Zylstra CR, Alenina N, Robinson DR, et al. Lrp5 functions in bone to regulate bone mass. *Nat Med* 2011;17:684–91.
- [16] Joeng KS, Schumacher CA, Zylstra-Diegel CR, Long F, Williams BO. Lrp5 and Lrp6 redundantly control skeletal development in the mouse embryo. *Dev Biol* 2011;359:222–9.
- [17] Stevens JR, Miranda-Carboni GA, Singer MA, Brugger SM, Lyons KM, Lane TF. Wnt10b deficiency results in age-dependent loss of bone mass and progressive reduction of mesenchymal progenitor cells. *J Bone Miner Res* 2010;25:2138–47.
- [18] Li X, Ominsky MS, Niu QT, Sun N, Daugherty B, D'Agostin D, et al. Targeted deletion of the sclerostin gene in mice results in increased bone formation and bone strength. *J Bone Miner Res* 2008;23:860–9.
- [19] Morvan F, Bouloukos K, Clement-Lacroix P, Roman Roman S, Suc-Royer I, Vayssiere B, et al. Deletion of a single allele of the Dkk1 gene leads to an increase in bone formation and bone mass. *J Bone Miner Res* 2006;21:934–45.
- [20] Gong Y, Slee RB, Fukai N, Rawadi G, Roman-Roman S, Reginato AM, et al. LDL receptor-related protein 5 (LRP5) affects bone accrual and eye development. *Cell* 2001;107:513–23.
- [21] Boyden LM, Mao J, Belsky J, Mitzner L, Farhi A, Mitnick MA, et al. High bone density due to a mutation in LDL-receptor-related protein 5. *N Engl J Med* 2002;346:1513–21.
- [22] Little RD, Carulli JP, Del Mastro RG, Dupuis J, Osborne M, Folz C, et al. A mutation in the LDL receptor-related protein 5 gene results in the autosomal dominant high-bone-mass trait. *Am J Hum Genet* 2002;70:11–9.
- [23] Babij P, Zhao W, Small C, Kharode Y, Yaworsky PJ, Bouxsein ML, et al. High bone mass in mice expressing a mutant LRP5 gene. *J Bone Miner Res* 2003;18:960–74.
- [24] Rodda SJ, McMahon AP. Distinct roles for Hedgehog and canonical Wnt signaling in specification, differentiation and maintenance of osteoblast progenitors. *Development* 2006;133:3231–44.
- [25] Day TF, Guo X, Garrett-Beal L, Yang Y. Wnt/beta-catenin signaling in mesenchymal progenitors controls osteoblast and chondrocyte differentiation during vertebrate skeletogenesis. *Dev Cell* 2005;8:739–50.
- [26] Hill TP, Spater D, Taketo MM, Birchmeier W, Hartmann C. Canonical Wnt/beta-catenin signaling prevents osteoblasts from differentiating into chondrocytes. *Dev Cell* 2005;8:727–38.
- [27] Wei W, Zeve D, Suh JM, Wang X, Du Y, Zerwekh JE, et al. Biphasic and dosage-dependent regulation of osteoclastogenesis by beta-catenin. *Mol Cell Biol* 2011;31:4706–19.
- [28] Yadav VK, Ryu JH, Suda N, Tanaka KF, Gingrich JA, Schutz G, et al. Lrp5 controls bone formation by inhibiting serotonin synthesis in the duodenum. *Cell* 2008;135:825–37.
- [29] Takada I, Mihara M, Suzawa M, Ohtake F, Kobayashi S, Igarashi M, et al. A histone lysine methyltransferase activated by non-canonical Wnt signalling suppresses PPAR-gamma transactivation. *Nat Cell Biol* 2007;9:1273–85.
- [30] Tu X, Joeng KS, Nakayama KI, Nakayama K, Rajagopal J, Carroll TJ, et al. Noncanonical Wnt signaling through G protein-linked PKCdelta activation promotes bone formation. *Dev Cell* 2007;12:113–27.
- [31] Bennett CN, Longo KA, Wright WS, Suva LJ, Lane TF, Hankenson KD, et al. Regulation of osteoblastogenesis and bone mass by Wnt10b. *Proc Natl Acad Sci USA* 2005;102:3324–9.
- [32] Bennett CN, Ouyang H, Ma YL, Zeng Q, Gerin I, Sousa KM, et al. Wnt10b increases postnatal bone formation by enhancing osteoblast differentiation. *J Bone Miner Res* 2007;22:1924–32.
- [33] Kim JB, Leucht P, Lam K, Luppen C, Ten Berge D, Nusse R, et al. Bone regeneration is regulated by Wnt signaling. *J Bone Miner Res* 2007;22:1913–23.
- [34] Maeda K, Kobayashi Y, Udagawa N, Uehara S, Ishihara A, Mizoguchi T, et al. Wnt5a-Ror2 signaling between osteoblast-lineage cells and osteoclast precursors enhances osteoclastogenesis. *Nat Med* 2012;18:405–12.
- [35] Styrkarsdottir U, Halldorsson BV, Gudbjartsson DF, Tang NL, Koh JM, Xiao SM, et al. European bone mineral density loci are also associated with BMD in East-Asian populations. *PLoS One* 2010;5:e13217.
- [36] Rivadeneira F, Styrkarsdottir U, Estrada K, Halldorsson BV, Hsu YH, Richards JB, et al. Twenty bone-mineral-density loci identified by large-scale meta-analysis of genome-wide association studies. *Nat Genet* 2009;41:1199–206.
- [37] Fu J, Ivy Yu HM, Maruyama T, Miranda AJ, Hsu W. Gpr177/mouse Wntless is essential for Wnt-mediated craniofacial and brain development. *Dev Dyn* 2011.
- [38] Zhu X, Zhu H, Zhang L, Huang S, Cao J, Ma G, et al. Wls-mediated Wnts differentially regulate distal limb patterning and tissue morphogenesis. *Dev Biol* 2012.
- [39] Fu J, Jiang M, Miranda AJ, Yu HM, Hsu W. Reciprocal regulation of Wnt and Gpr177/mouse Wntless is required for embryonic axis formation. *Proc Natl Acad Sci USA* 2009;106:18598–603.
- [40] Myung PS, Takeo M, Ito M, Atit RP. Epithelial Wnt ligand secretion is required for adult hair follicle growth and regeneration. *J Invest Dermatol* 2012.
- [41] Zhong Z, Zylstra-Diegel CR, Schumacher CA, Baker JJ, Carpenter AC, Rao S, et al. Wntless functions in mature osteoblasts to regulate bone mass. *Proc Natl Acad Sci USA* 2012;109:E2197–204.
- [42] Zha L, Hou N, Wang J, Yang G, Gao Y, Chen L, et al. Collagen1alpha1 promoter drives the expression of Cre recombinase in osteoblasts of transgenic mice. *J Genet Genomics* 2008;35:525–30.
- [43] Tan X, Weng T, Zhang J, Wang J, Li W, Wan H, et al. Smad4 is required for maintaining normal murine postnatal bone homeostasis. *J Cell Sci* 2007;120:2162–70.
- [44] Dacquin R, Starbuck M, Schinke T, Karsenty G. Mouse alpha1(I)-collagen promoter is the best known promoter to drive efficient Cre recombinase expression in osteoblast. *Dev Dyn* 2002;224:245–51.
- [45] Harada N, Tamai Y, Ishikawa T, Sauer B, Takaku K, Oshima M, et al. Intestinal polyposis in mice with a dominant stable mutation of the beta-catenin gene. *EMBO J* 1999;18:5931–42.
- [46] Bouxsein ML, Boyd SK, Christiansen BA, Guldberg RE, Jepsen KJ, Muller R. Guidelines for assessment of bone microstructure in rodents using micro-computed tomography. *J Bone Miner Res* 2010;25:1468–86.
- [47] Jacquin C, Gran DE, Lee SK, Lorenzo JA, Aguila HL. Identification of multiple osteoclast precursor populations in murine bone marrow. *J Bone Miner Res* 2006;21:67–77.
- [48] Feng X, McDonald JM. Disorders of bone remodeling. *Annu Rev Pathol* 2011;6:121–45.
- [49] Mendez-Ferrer S, Michurina TV, Ferraro F, Mazloom AR, MacArthur BD, Lira SA, et al. Mesenchymal and haematopoietic stem cells form a unique bone marrow niche. *Nature* 2010;466:829–34.
- [50] Zhang M, Xuan S, Bouxsein ML, von Stechow D, Akeno N, Faugere MC, et al. Osteoblast-specific knockout of the insulin-like growth factor (IGF) receptor gene reveals an essential role of IGF signaling in bone matrix mineralization. *J Biol Chem* 2002;277:44005–12.
- [51] Boban I, Jacquin C, Prior K, Barisic-Dujmovic T, Maye P, Clark SH, et al. The 3.6 kb DNA fragment from the rat Col1a1 gene promoter drives the expression of genes in both osteoblast and osteoclast lineage cells. *Bone* 2006;39:1302–12.
- [52] Coskun S, Hirschi KK. Establishment and regulation of the HSC niche: roles of osteoblastic and vascular compartments. *Birth Defects Res C Embryo Today* 2010;90:229–42.